CHAPTER IV

RESULTS

CCNA1 methylation in CC cell lines

Many reports found that *CCNA1* was methylated in HeLa cell (15,94). To confirm this particular finding in CC cell lines, we investigated methylation and expression in HeLa and SiHa cells. Our preliminary study in HeLa, HeLa(S), revealed complete non-methylation, which contradicts the previous report (Figure 8). To settle this controversy, we attempted to further evaluate additional CC cell lines, including HeLa(K) grown in a different laboratory, and SiHa. The result confirmed the previous finding. The majority of Hela(K) cells, as well as all SiHa cells, were hypermethylated. *CCNA1* RT-PCR confirmed the inverse relation between DNA methylation and gene expression. *CCNA1* RNA levels were high, intermediate and low in HeLa(S), HeLa(K) and SiHa cells, respectively (Figure 8). These data indicate that *CCNA1* methylation is common in CC cell lines and its physiological role is to decrease gene expression.

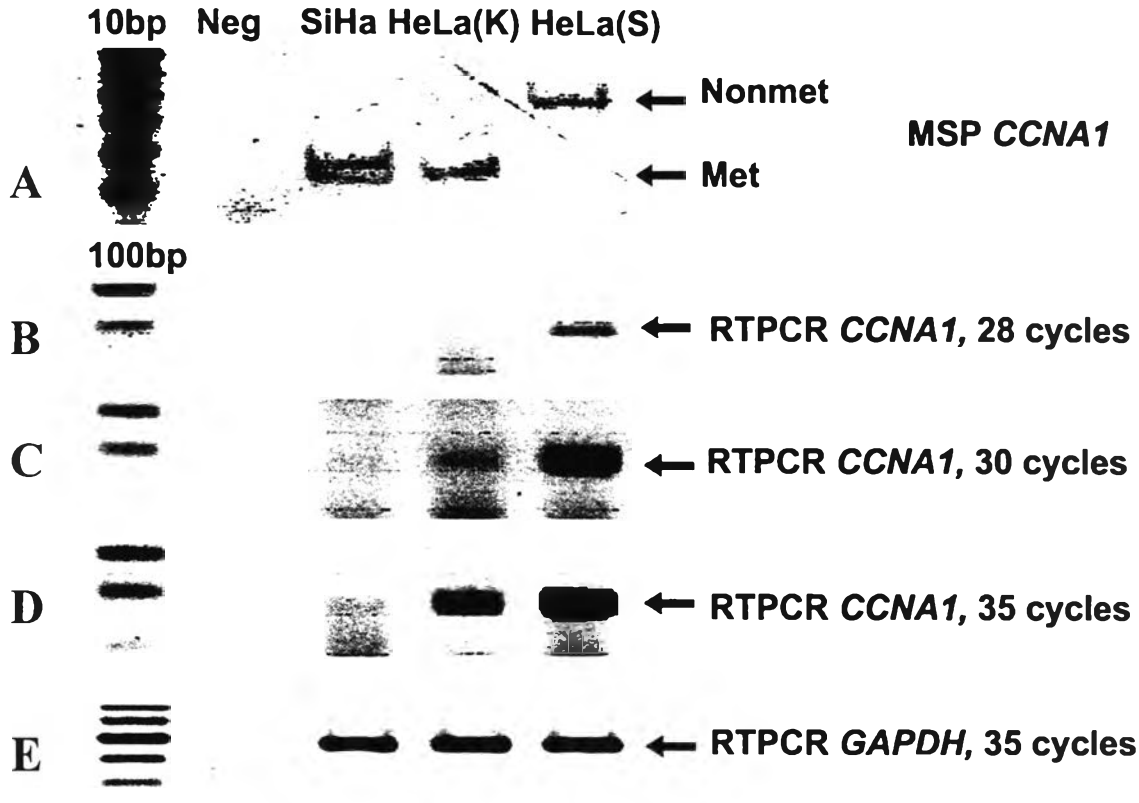

Figure 8. Schematic representation of inverse correlation between promoter methylation and expression of *CCNA1* in CC cell lines: M, DNA size marker. Top panel, 10-bp ladder; bottom four panels, 100-bp ladder. Neg, negative. (A) Duplex MSP analysis of cell lines. Upper and lower arrows indicate non-methylated and methylated amplicons, respectively. MSP, methylation-specific PCR. (B-D) RT-PCR of the *CCNA1* gene after 28, 30 and 35 cycles, respectively. (E) RT-PCR of the *GAPDH* gene as an internal control. M, DNA size marker. Top panel, 10-bp ladder; bottom four panels, 100-bp ladder. Neg, negative.

Reliability validation of this duplex MSP was performed by calibration experiments. Using SiHa mixed with HeLa(S) which *CCNA1* completely hypermethylated and non-methylated cells, respectively (Figure 9). With at least three replicates for each experiment, after measured methylation and non methylation band with Storm 840 and ImageQuaNT solfware (Molecular dynamics), the result demonstrates the consistency of the current approach, with minimal intra- and inter-assay variations (Figure 10). It is noteworthy that the correlation between measured and actual *CCNA1* methylation percentages was not linear, but exponential. We can calculated the actual methylated PCR products Because according to the formula: $Y=2.145e^{0.0391X}$ (Y=measured methyaltion, X=actual methylation) (Figure 11)

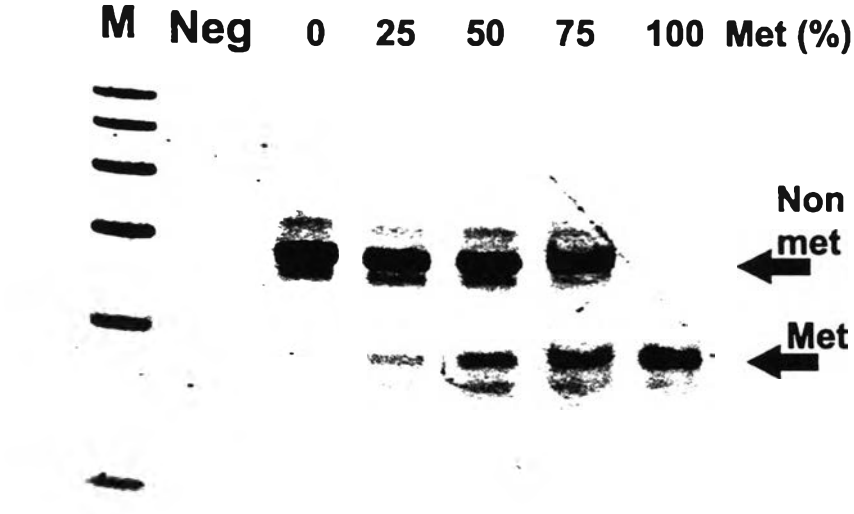

Figure 9. Intra- and inter-assay variation of the duplex MSP. Duplex MSP of a mixture of *CCNA1* complete and non-methylated CC cell lines, SiHa and HeLa(S), respectively. M, DNA size marker; Neg, negative; 0, 25, 50, 75, 100 Met (%) represent the proportion of SiHa DNA in the mixture, varied from 0 to 100%, respectively. The upper and lower bands are non-methylated and methylated bands, respectively, indicated by labeled arrows.

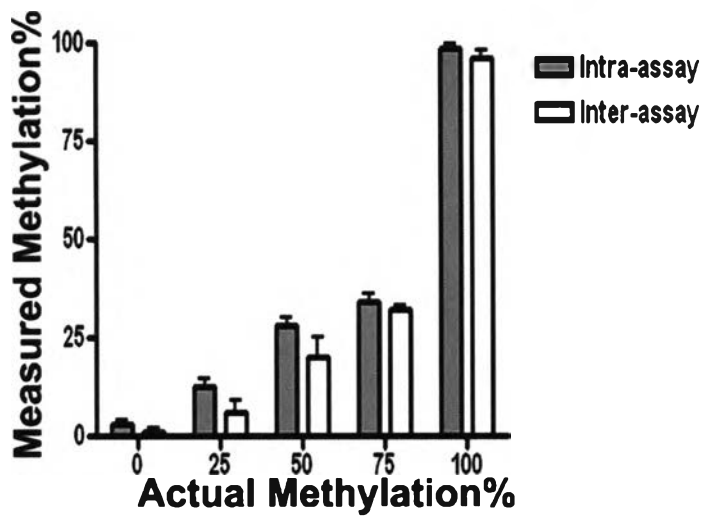

Figure 10. Bar graph of MSP intra- and inter-assay variation. Graphical comparison between measured *CCNA1* methylation, percentage intensity of methylation amplicon (x-axis), and actual methylation, the proportion of SiHa DNA (y-axis). The bar height indicates the mean and error bars represent ranges across experiments.

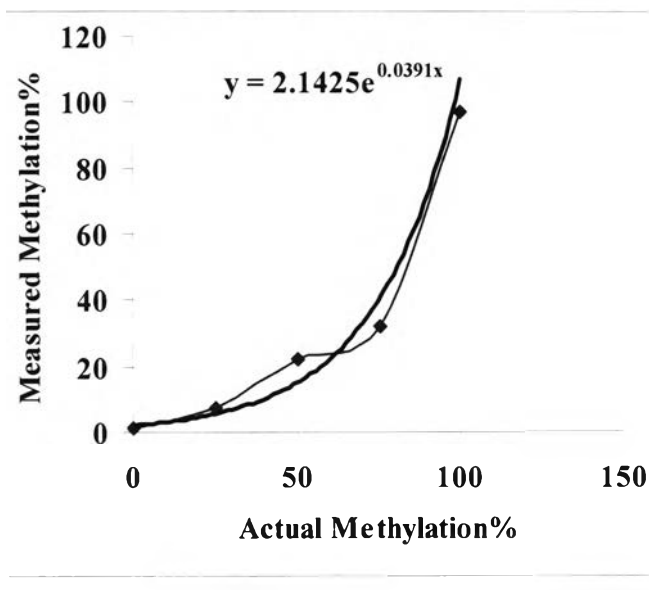

Figure 11. Exponential MSP graph curve and formula. Graphical comparison between measured *CCNA1* methylation, percentage intensity of methylation amplicon (x-axis), and actual methylation, the proportion of SiHa DNA (y-axis). The formula calculated after adjust the curve.

CCNA1 methylation and expression in cervical tissues

We expected the outcome of *in vivo* study possibility has the same situation as *in vitro*. We evaluated 6 frozen OTC-embedded CCs and five normal cervices, By microdissected, DNA, RNA extraction and subjected to duplex MSP and *CCNA1* RT-PCR. The results was shown that, First, whereas no methylation could be observed, *CCNA1* mRNA was discoverable by RT-PCR in normal cervix from both epithelium and connective tissue cells (Figure 12). In contrast, methylated band was detectable in cervical epithelia of CC patients from both malignant cells and adjacent histologically normal cervical epithelia . Nonetheless, in matched cases, a higher degree of methylation could be demonstrated in cancer than in normal cells. From all CCs, no *CCNA1* mRNA was detectable. Interestingly, even if methylation was detected, *CCNA1* was expressed in malignancy-adjacent histologically normal cervical tissues. Moreover, an inverse correlation between the methylation level and mRNA quantity was observed. After genomic sequencing analysis, 17 of CG positions was investigated and displayed in Figure 13 (complete methylation) and Figure 14 (complete non methylation) Whereas complete methylation could be observed in most cancer cells, partial and non-methylated *CCNA1* was discovered in the adjacent epithelia (Figure 15).

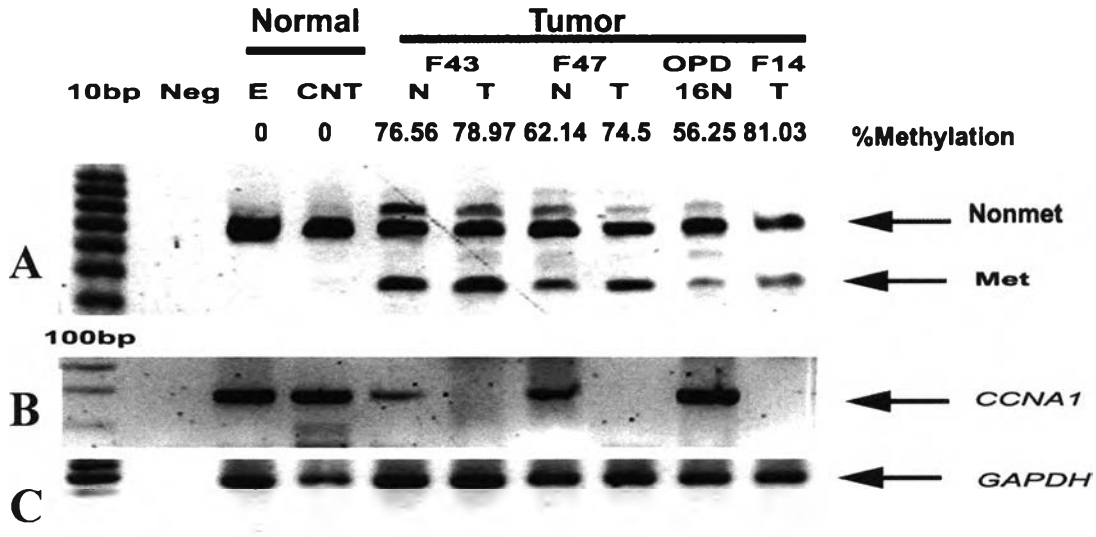

Figure 12. *CCNA1* methylation and expression in microdissected cervical tissues. (A) Duplex MSP and *CCNA1* PCR; E and CNT are epithelium and connective tissue cells from normal cervix; N and T are adjacent histological normal and cancer cervical epithelium from CC, respectively. Arrows indicate non-methylated, methylated, *CCNA1* cDNA and *GAPDH* cDNA, respectively.

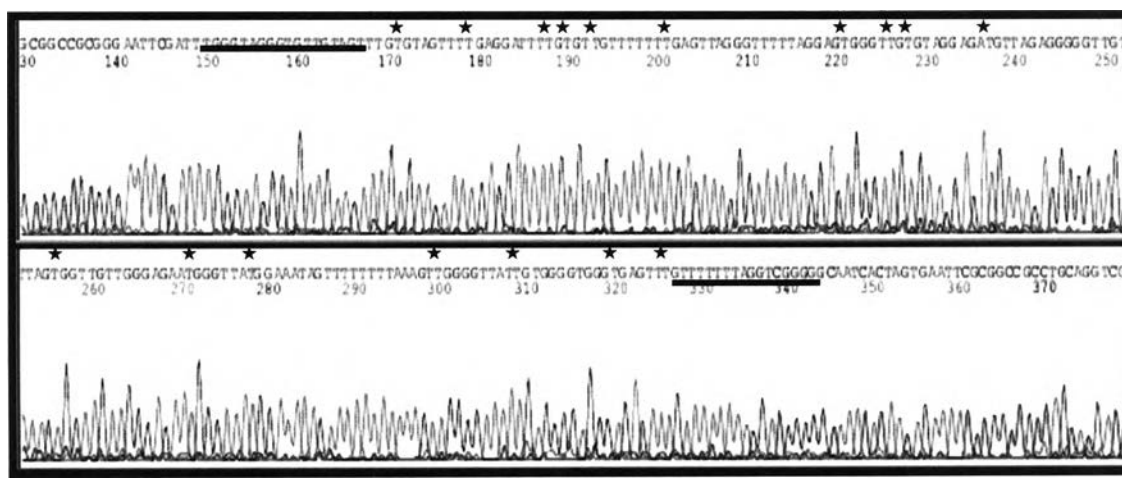

Figure 13. Sample of bisulfite *CCNA1* sequence from normal cervix. Each * indicates non -methylated CGs. PCR primer positions are underlined.

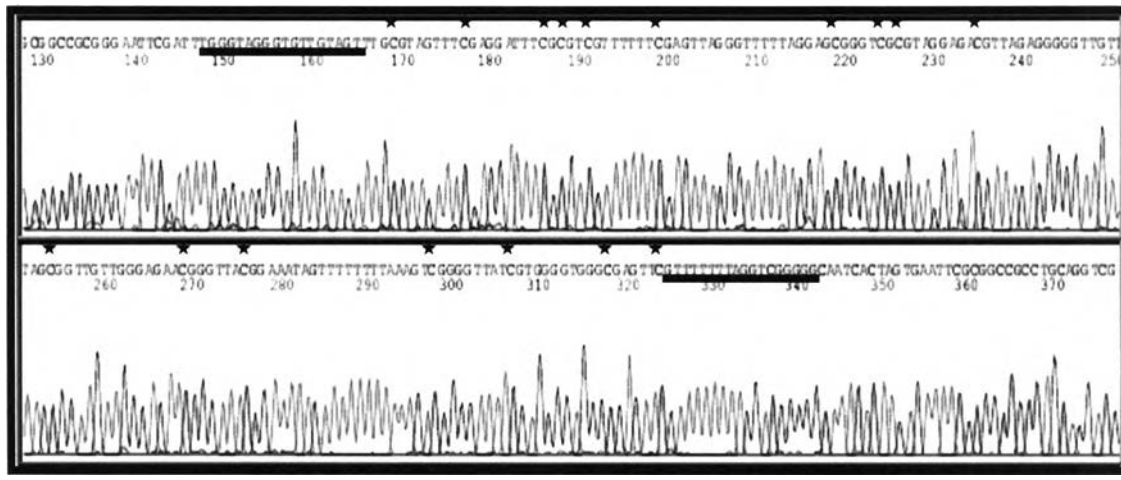

Figure 14. Sample of bisulfite *CCNA1* sequence from CC. Each * indicates methylated CGs. PCR primer positions are underlined.

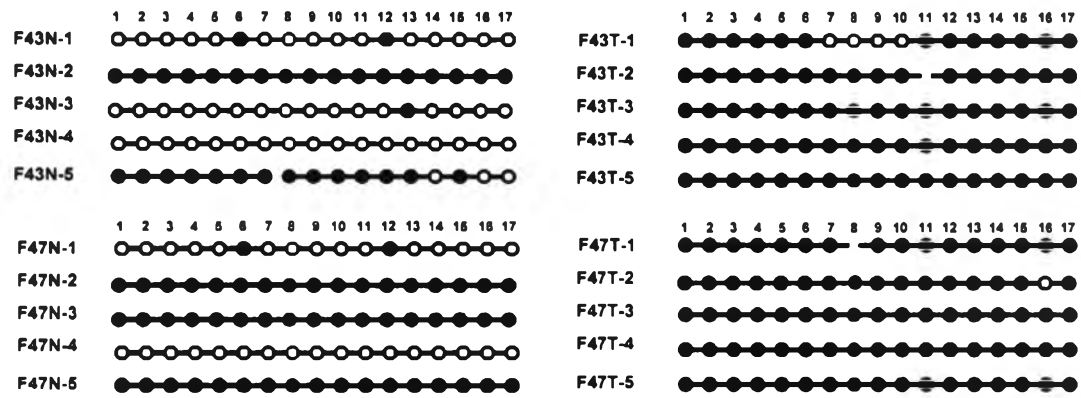

Figure 15. Bisulfite sequencing at the *CCNA1* promoter, with circles denoting the methylation status of each selected clone. Black and white circles are methylated CG dinucleotides, and non-methylated CpG dinucleotides and TG dinucleotides, respectively.

CCNA1 methylation incidence during multistep cervical carcinogenesis

Cervical intraepithelial neoplasia provides a crucial model to study the multistep process of carcinogenesis. Therefore, we evaluated the frequency of *CCNA1* methylation in several cervical epithelial tissues with a distinctive degree of malignant transformation, normal cervix, CIN, microinvasive and CC, respectively. We selected 43, 25 and 30 cases of white blood cells (WBC), normal cervical biopsies and invasive CCs, respectively (Table 3). Among these samples, 13 WBC samples and 6 normal cervical samples, located at least 3 cm from the tumor margin and showing the absence of HPV DNA, originated from CC patients. For all cases, when a methylated amplicon was visible and the methylation percentage measured exceeded 5%, the test was deemed positive. All selected CCs were squamous (keratinized 9 cases, nonkeratinized 21 cases) and positive for HPV. Of the cases, 24 harbored HPV type 16, 4 had HPV type 18 and 2 cases displayed unclassifiable HPV types. Interestingly, a high frequency of methylation was exclusively present in CCs, i.e., 28 cases or 93.3%, classified to KSCC 9 cases (90%), NKSCC 19 cases (90.5%). (Figure 16, 17 ,Table 3, 4, 5)

Furthermore, we also observed the *CCNA1* methylation in adenocarcinoma and adenosquamous cell carcinoma. This methylation was found 7 in 9 cases (78%) and 1 in 3 cases (33.3%) in adenocarcinoma and adenosquamous cell carcinoma respectively. (Table 6, 7)

To reveal multistep carcinogenesis, we included 24 cases of SILs and 5 microinvasive cancers from exfoliated cervical cells. All cases were positive for oncogenic HPV, analyzed by Hybrid Capture 2. Whereas 60% and 36.6% of the microinvasive cancers and high SILs, respectively, demonstrated *CCNA1* methylation, none of the HPV-associated low SILs exhibited these epigenetic changes (Figure 17 and Table 3).

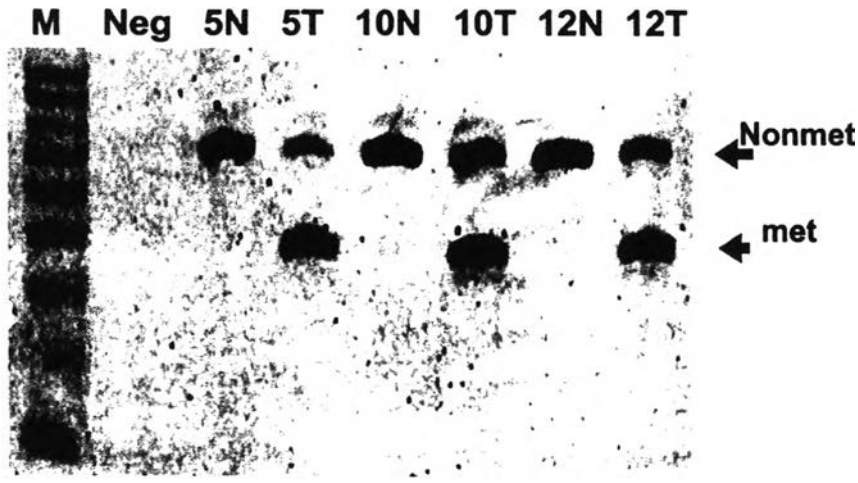

Figure 16. Schematic representation of methylation-specific PCR in CC. (A) PCR analysis of CC: M, DNA size marker; Neg, water; N and T, matched normal cervices and tumors, respectively.

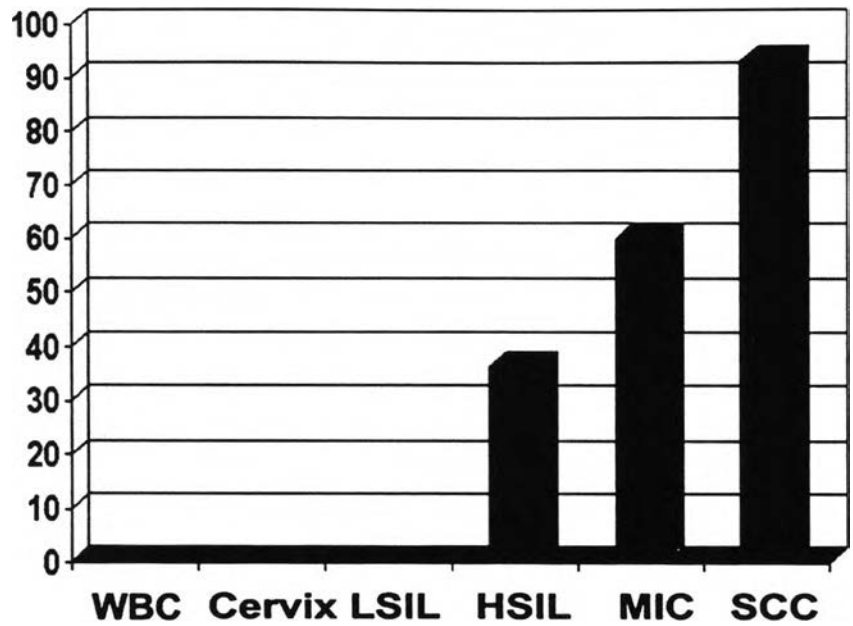

Figure 17. Bar graph demonstrating the frequency of DNA methylation in cervical carcinogenesis. Numbers on the y-axis are the percentage of positive methylation cases. Sample types are on the x-axis. The methylation frequencies of each tissue type are represented by the height of each rectangular bar.

Table 3. *CCNA1* methylation and clinico-pathological correlation

Histological characteristics	Total number of cases	*CCNA1* promoter hypermethylation	
		Absent	Present
WBC	43	43	0
Normal cervix	25	25	0
Low-grade SIL	13	13	0
High-grade SIL	11	7	4
Microinvasive cancer	5	2	3
Squamous cell CC	30	2	28
FIGO stage I–IIA	6	0	6
FIGO stage IIB–IV	24	2	22
Grade 1, keratinized type	9	0	9
Grade 2, non-keratinized type	21	2	19

FIGO, International Federation of Gynecology and Obstetrics.

CCNA1 methylation and clinicopathological correlations

We tried to explore the correlation between methylation status of the cyclin A1 gene with HPV infection, pathological grade, FIGO staging (Appendix E) and treatment outcome (Table 4-7). Cause of nonmethylation population only have 2 cases , lead to limited in evaluate the correlation. No statistic significant correlation of each condition was observed.

Table 4. *CCNA1* methylation in KSCC and clinical correlation

No	Age	Staging	HPV	*CCNA1*	Survival
C1	52	3B	16	Met	NED
C23	57	2B	16	Met	NED
CX18	52	3B	16	Met	Metas
CX23	50	2B	16	Met	Recur, Metas
CX24	47	3B	16	Met	NED
CX25	62	1B	16	Met	NED
CX50	48	3B	16	Met	NED
OPD1	42	3B	18	Met	Recur
OPD12	31	3B	16	Met	Dead

NED, No evidence of disease ; F/U, follow up

Table 5. *CCNA1* methylation in NKSCC and clinical correlation

No	Age	Staging	HPV	*CCNA1*	Survival
C11	57	3B	16	Met	LostF/U
C12	50	2B	16	Met	NED
C13	69	3B	16	Met	LostF/U
C19	55	3B	16	Met	LostF/U
C26	35	2B	16	Met	NED
C42	57	3B	16	Met	Dead
C55	41	1B	16	Met	NED
C104	35	2B	16	Met	LostF/U
C119	48	1B	16	Met	NED
CX5	58	2B	16	Met	NED
CX8	63	3B	16	Met	Metas
CX9	46	3B	16	Met	dead
CX11	37	2B	16	Met	NED
CXF23	41	1B1	16	Met	NED
CXF27	47	1A2	other	Met	NED
CXF29	53	1B	18	Met	Recur
OPD6	80	3B	16	Met	Dead
OPD18	54	3B	other	Met	NED
OPD20	47	2B	16	Met	NED
CX14	49	3B	18	Nonmet	Recur, Metas
OPD13	47	3B	18	Nonmet	NED

NED, No evidence of disease ; F/U, follow up

Table 6. *CCNA1* methylation in adenocarcinoma and clinical correlation

No	Age	Staging	HPV	*CCNA1*	Survival	Grade
C79	41	1B	16	Met	NED	Unknown
C118	30	1B	16	Met	Lost F/U	WD
CX12	44	3B	16	Met	Lost F/U	PD
CX15	51	2B	16	Met	Lost F/U	WD
CXF34	41	1B	16	Met	NED	WD
CXF45	72	1B	16	Met	NED	WD
OPD5	38	2B	18	Met	Lost F/U	MD
CXF32	67	1B	16	Nonmet	NED	WD
OPD16	56	3B	other	Nonmet	NED	WD

WD, well differentiated; MD,moderate differentiated; PD,poorly differtiated;

NED, No evidence of disease ; F/U, follow up

Table 7. *CCNA1* methylation in adenosquamous cell carcinoma and clinical correlation

No	Age	Staging	HPV	*CCNA1*	Survival	Grade
CXF47	27	1B	16	Nonmet	Dead	PD
OPD15	37	3B	18	Nonmet	NED	PD
OPD19	42	3B	16	Met	NED	MD

MD,moderate differentiated; PD,poorly differtiated;NED, No evidence of disease ; F/U, follow up

CCNA1 methylation and HPV Status

Some of CC tissues were evaluate for quantity of HPV by comparing L1 HPV gene per Hat exon 4 gene and percentage of methylation. No correlation of both parameter was observed statistical significantly (Linear regression P=0.172 (95% CI) , Spearman's rho test: R square= 0.047) , as shown in table 8, 9 and figure 18. Fortunately when we classified to episome group and integrated group followed HPV status, the percent of CCNA1 methylation compare to ratio of L1/Hat exon 4 gene was displayed statistically significant(Independent sample T- test P=0.037, 95% CI= 5.86 to -2.20)

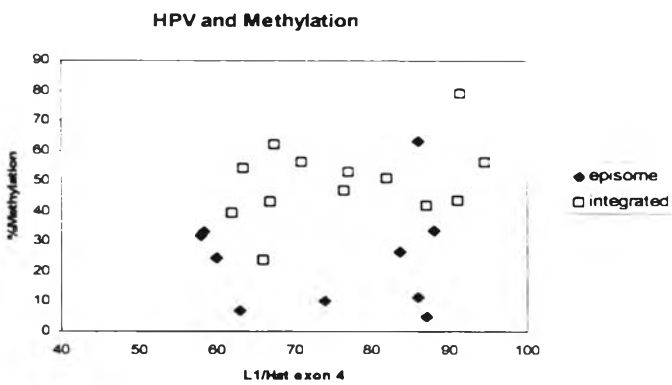

Figure 18. Graph demonstrating the *CCNA1* methylaion and HPV morphology. Graphical comparison between the proportion of HPV L1/Hat exon 4 DNA (X-axis) and percentage intensity of methylation amplicon (y-axis) indicates

Table 8. Percentage of *CCNA1* methylation in CC (HPV integrated form)

Integrated	L1/Hat exon4	%Met
CX23	63.5	54
CX50	66	24
C1	82	51
CXF29	76.5	47
C119	62	39.5
CXOPD12	71	56
C13	94.5	56
C26	87	42
C104	67	43
C23	91	43.5
C42	77	53
C6	91.5	79
C69	67.5	62

Table 9. Percentage of *CCNA1* methylation in CC (HPV episomal form)

Episome	L1/Hat exon4	%Met
CXF23	58.5	33.5
CX8	58	32
CX11	63	7
CX25	60	25
CX9	87	5
CX5	88	34
C12	83.5	27
C19	86	11.5
C11	86	63
C55	74	10